Journal of Alloys and Compounds 676 (2016) 80–85

Contents lists available at ScienceDirect

Journal of Alloys and Compounds

journal homepage: http://www.elsevier.com/locate/jalcom

Grain coarsening and its effects on the properties of magnetoelectric $0.675(Pb(Mg_{1/3}Nb_{2/3})O_3)-0.325PbTiO_2/CoFe_2O_4$ particulate composites

F.L. Zabotto [a, *], A.J. Gualdi [b], P.C. de Camargo [b], A.J.A. de Oliveira [b], J.A. Eiras [a], D. Garcia [a]

[a] Group of Ferroic Materials, Department of Physics, Federal University of São Carlos, São Carlos, SP, CEP 13565-905, Brazil
[b] Group of Superconductivity and Magnetism, Department of Physics, Federal University of São Carlos, São Carlos, SP, CEP 13565-905, Brazil

ARTICLE INFO

Article history:
Received 14 December 2015
Received in revised form
19 February 2016
Accepted 9 March 2016
Available online 12 March 2016

Keywords:
Grain size effect
Magnetoelectric properties
PMN-PT
Ferroelectric

ABSTRACT

In this work, the influence of the grain coarsening on dielectric, magnetic and magnetoelectric properties of particulate composites constituted by $(0.8)0.675(Pb(Mg_{1/3}Nb_{2/3})O_3)-0.325PbTiO_2 - (0.2)CoFe_2O_4$ (or PMNPT-CFO) and prepared by solid-state reaction method are presented. The increase of average grain size enhances the tetragonal distortion at the structure of the PMNPT matrix due to control of internal stress of the ferroelectric phase. As consequence, the values of the ε', g_{33} and α_{ME} coefficients reached maximum ($\varepsilon' = 25{,}000$, $g_{33} = 53 \times 10^{-4}$ Vm/N and $\alpha_{ME} = 14.5$ mV/cm Oe) as result of the enhancement of domain structure in the composites. An increase of aprox. 65% in the magnetoeletric coefficient was achieved controlling the microstructure of composites indicating that the magnetoelectric properties in these composites systems could be enhanced by the correct control of the grain coarsening between the phases in particulate composites.

1. Introduction

Important advances in materials science are critical for the development of new technologies. Multiferroic materials are very promising candidate for the design of novel devices since they present two or more switchable states such electric polarization, magnetization or strain [1,2]. The interplay between electric and magnetic states is realized through the magnetoelectric effect (ME), which is defined as the coupling between electric and magnetic fields in matter [2]. This coupling is generally classified as direct or indirect, depending on the material type. Direct coupling is achieved in single-phase materials, in which generally is the result of a direct interaction between electric and magnetic moment in the matter, but the realizable magnitude of the ME signals as well as the operation temperature is still not sufficient for practical applications [3,4]. On the other hand, an indirect coupling can be mediated by strain to couple electric and magnetic moments in the matter. In this sense, composites system may be used to generate magnetoelectric effect by means of the product properties concept. In this case, the ME effect is obtained by the interaction between piezoelectric and magnetostrictive (or piezomagnetic) properties through the indirect mechanical interaction at interface of different phases in composite. Therefore, an investigation of the influences of parameters as processing routes, connectivity, grains size and constituent phases becomes important for the enhancement of the ME coupling in composites systems [3–7]. For composites materials that exhibits 0–3 connectivity (also called particulate composites) it could be detached many advantages in comparison to the other connectivity, mainly due to the low cost and easiness of the fabrication added to the possibility of the control the piezoelectric/magnetostrictive phase molar ratio and the grain size of each phase [8–13]. In addition, it is expected to obtain high ME response since the contact between phases is enhanced in 0–3 connectivity [4]. Actually, novel composites using lead titanate modified lead magnesium niobate, or PMNPT, as piezoelectric phase, has been studied due to their improved piezoelectric properties, compared to the PZT ceramics. For bulk 0–3 PMNPT based composites, it was reported values of the ME coefficient between 0.1 and 30 mV/cm Oe, which is high in comparison with those of the PZT based ones [14–17]. Differences between the reported values are mainly related to the microstructure and electrical resistivity of the composites [14–17]. Since it is well known that the coarsening of the microstructure influences the piezoelectric, dielectric and

* Corresponding author.
E-mail address: zabotto@df.ufscar.br (F.L. Zabotto).

http://dx.doi.org/10.1016/j.jallcom.2016.03.050
0925-8388/

ferroelectric properties of the ferroelectric materials [18–20], it is necessary a systematic study of the influences of coarsening in microstructures on the ME voltage coefficient for PMNPT/CFO particulate composites. In these systems, a decrease in the average grain size is accomplished by the increasing of the compressive stress on the inner part of a grain and this effect plays an important role in ferroelectric and piezoelectric properties [18–20]. Particularly for the case of the ferroelectric PMNPT (32% molar of PT) ceramics it is known that a grain size tuning allows the control of the tetragonal distortion of its perovskite unit cell [19], affecting the overall ferroelectric domain dynamics and net polarization. In addition, a recent theoretical study suggest that it is possible to manipulate the material microstructure scale for designing magnetoelectric composites with different properties according to design requirements [21]. Therefore, this work analyses the effect of grain coarsening on the structural, dielectric and magnetic properties of PMNPT/CFO particulate composites and its influences on the magnetoelectric coupling.

2. Experimental procedures

Magnetoelectric composites of PMNPT and $CoFe_2O_4$ (CFO) were prepared by the solid-state reaction method. The cobalt ferrite (CFO) ceramic powder was prepared by using Co_3O_4 and Fe_2O_3 as starting materials. The powders were mixed through ball-milling (in distilled water with ZrO_2 cylinders), calcined at 900 °C, for 4 h, and then, grinded (again by ball milling), for 10 h. The PMNPT powder, with nominal formula (1-y) (Pb $(Mg_{1/3}Nb_{2/3})O_3 - yPbTiO_3$ (y = 0.325), was obtained by the Columbite Method. The columbite precursor, $MgNbO_6$ (MN) was prepared from MgO and Nb_2O_5 mixed oxides, and calcined at 1100 °C, for 4 h. Then, following the batching formula, MN precursor was mixed with PbO and TiO_2, calcined at 900 °C, for 4 h, and ball milling grinded for 10 h. The ball milled composite powders of (0.8) $[0.675Pb(Mg_{1/3}Nb_{2/3})O_3–0.325PbTiO_2] + 0.2CoFe_2O_4$ (herein after PMNPT/CFO) were uniaxially and hydrostatic cold-pressed into pellets (~10 mm in diameter and ~2 mm thick) using a hydraulic press and sintered for different sintering times (1–15 h) at optimized temperature of 1050 °C. The phase identification of the fired specimens was performed through X-ray diffraction (XRD) using a Rigaku Rotaflex RU200B diffractometer, with CuK_α radiation 2θ from 20 to 60°, 2°/min. The apparent density (ρ_{app}) was obtained using an apparatus based on the Archimedes principle, with distilled water as immersion liquid. A Jeol 5400 LV microscope was used for the scanning electron microscopy characterization of the optically polished and thermally etched samples surfaces. The grain size of the ferroelectric and ferrite phase was determined based on microstructures through the line intercept method. Dielectric properties characterization was performed on samples with gold sputtered surfaces using an HP 4194A impedance gain phase analyzer. The measurements were performed over a temperature range of 300 K < T < 800 K, during cooling at a constant rate of 2 K/min. The fitting of ε' versus T curves around and above ferroelectric-paraelectric temperature phase transition (Tm) was performed using a phenomenological equation, called Santos–Eiras expression [21]. The parameters δ and ξ related to the transition diffuseness and to the character of the phase transition were adjusted by:

$$\varepsilon' = \frac{\varepsilon_m}{1 + \left(\frac{(T - Tm)}{\delta}\right)^{\xi}} \quad (1)$$

where δ, ξ, ε_m, ε', T_m and T are transition diffuseness, phase transition type coefficient, maximum value of electrical permittivity, real part of electrical permittivity, temperature at ε_m and temperature of measurement, respectively.

The dc electrical resistivity measurements, at room temperature, were taken using an electrometer (Keithley model 617). A Physical Properties Measurement System (PPMS) dc extraction magnetometer by Quantum Design (model 7100) was used to measure the magnetic hysteresis, at 300 K, up to 50 kOe. A homebuilt sensor based on the capacitive cell was used in the PPMS to measure the magnetostrictive curves, at 300 K, up to 6 kOe. The composites were poled at 20 kV cm^{-1}, for 30 min, at room temperature and the voltage piezoelectric coefficient g_{33} was determined by the resonance method, at 300 K. The longitudinal magnetoelectric voltage coefficient (α_{ME}) was determined from the magnetic field induced voltage, measured across the sample using a lock in amplifier. In this case, a bias magnetic field up to 0.8T was applied overlapped by ac magnetic field of 2 Oe at 1 kHz.

3. Results and discussion

Fig. 1 shows the x-ray diffraction pattern of the PMNPT/CFO particulate composites sintered at different sintering time. The analyses of the XRD pattern reveal that the crystalline structure of the sintered composites are represented by the individual spinel cobalt ferrite CFO and perovskite PMNPT phase peaks, which unidentified peaks were not observed, indicating the absence of spurious phases. A splitting of the peaks related to the (00*l*) and (*h*00) planes (detailed in the Fig. 1), characteristic of the tetragonal symmetry of the perovskite structure, is observed with increasing the sintering time. The results of analysis of the *c*/*a* tetragonal ratio, volume cell of the perovskite PMNPT and the *a* CFO lattice parameter as a function of the sintering time are presented in Table 1. An increase of the *c*/*a* values from 1.004 to 1.011 with the sintering time, without significant changes in the volume cell of PMNPT lattice added to the invariance of the *a* lattice parameter of the CFO phase close to 8.41 Å, shows an enhancement of the tetragonal structural distortion without changes in the stoichiometry of phases. These evidences suggest that chemical reaction did not occur between PMNPT and ferrite phases during the sintering process.

The scanning electron microscopy (SEM) image of the composites sintered between 1 h and 15 h are shown in Fig. 2. The SEM

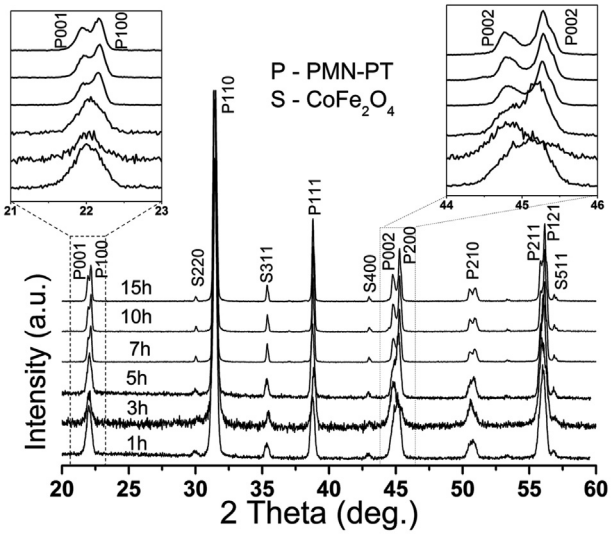

Fig. 1. XRD patterns of the PMNPT/CFO particulate composites for different sintering times (1 h–15 h), at 1050 °C. The 2θ intervals 20–26° and 42.5–47.5° are in featured to emphasize the tetragonal distortion enhancement with the sintering time.

Table 1
Lattice parameter for PMNPT and CFO phases, Relative density, Average grain size and Electric resistivity values for PMNPT/CFO particulate composites as a function of the sintering time.

Sintering time (h)	c/a_{Matrix}	a_{CFO} (Å)	Relative density (%)	Average grain size of PMNPT (μm)	Electric resistivity (10^9 Ω cm)	Lattice volume (Å^3)
1.0	1.004	8.40 ± 0.03	95.0 ± 0. 3	0.8 ± 0.03	2.0 ± 0.1	64.5
3.0	1.006	8.40 ± 0.02	95.3 ± 0.2	1.6 ± 0.03	2.2 ± 0.3	65.4
5.0	1.008	8.41 ± 0.02	95.8 ± 0.3	2.5 ± 0.03	2.4 ± 0.1	64.4
7.0	1.009	8.41 ± 0.03	96.8 ± 0.2	3.1 ± 0.03	1.0 ± 0.4	65.1
10.0	1.010	8.41 ± 0.02	97.2 ± 0.1	4.4 ± 0.03	0.93 ± 0.07	65.2
15.0	1.011	8.41 ± 0.04	97.2 ± 0.2	5.1 ± 0.03	0.27 ± 0.03	65.1

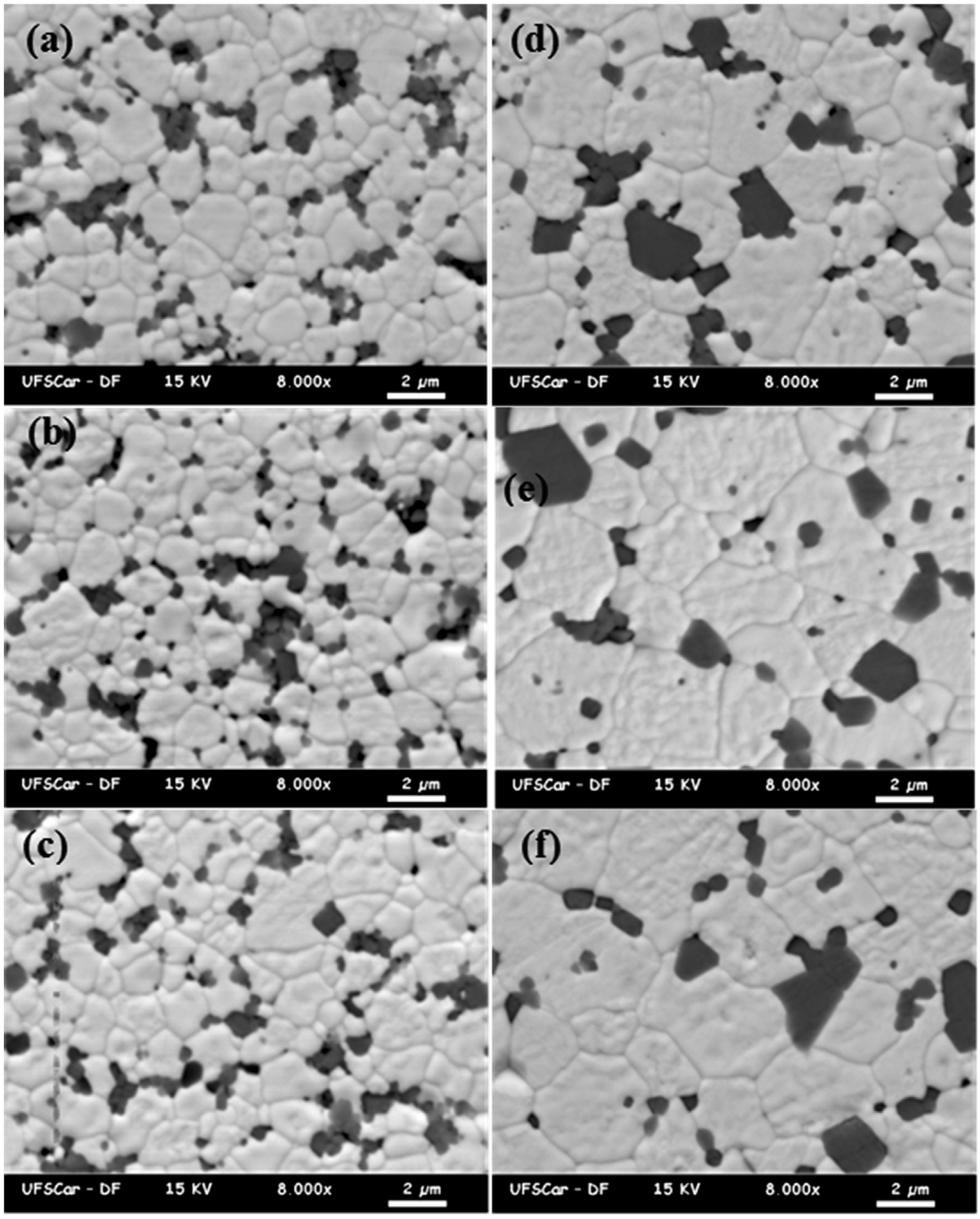

Fig. 2. SEM images of the polished surface of PMNPT/CFO particulate composites sintered at 1050 °C for different sintering times: (a) 1 h; (b) 3 h; (c) 5 h; (d) 7 h; (e) 10 h and (f) 15 h.

back scattering technique was employed to improve the image contrast between phases. Two distinct and well disperse phases can be easily identified, ferrite (dark) and ferroelectric phase (light in color). There is no large aggregation of the particles and the two phases are well distributed evidencing a 0–3 connectivity. Furthermore, the analyses of the micrographs confirm that the composites compounds exhibit a microstructure uniform without the presence of porosity, in agreement to the relative density values, higher than 95% of theoretical ones, as seen in the Table 1. Additionally, by increment the composites sintering time a

coarsening of PMNPT and CFO grains were observed, wherein for PMNPT phase the grain growth was from 0.8 μm to 5.0 μm, as also indicated in Table 1. For CFO grains, an increase from 0.8 μm to approx. 2 μm until 7 h of soaking time was observed, which this grain growth is clearly related to the growth of nearby CFO particles. After that, the average grain size shows a bimodal distribution for CFO grains, consisting of larger, with average grain size of ~2 μm, and smaller grains, localized mainly between the PMNPT grains, with an average grain size of the 1 μm. Such changes in the structure of ferroelectric matrix as well as in the distribution of ferrite and ferroelectric phases in composites, play a crucial role in the combined properties (magnetization, dielectric, etc.) and in the product properties such as the ME output [3,8].

In order to investigate the influence of the sintering time at the integrity between phases, dc electrical resistivity measurement of composites was carried, at room temperature, and the results are given in the Table 1. For all samples, a relatively high electric resistivity values (over 1×10^9 Ω cm) it was found in comparison with other values reported for similar magnetoelectric composites [10,12–14]. This improvement of resistivity is due to control the reaction between phases during to the sintering process. Based on these microstructural and electric resistivity properties obtained for sintered composites, it can be concluded that the inter-diffusion between phases was minimized. This is an important result in order to study the grain size effect, as it ensures that the difference of the electric, magnetic and magnetoelectric properties of composites comes mainly from the grain size differences, but not from others such as the impurity, porosity or inter-diffusion effects.

The real part of the dielectric permittivity, ε′, as a function of temperature, at 1 MHz, for PMNPT/CFO composites at different sintering time are shown in the Fig. 3. In all cases, the dielectric permittivity increases with increasing the measurement temperature from room temperature up to 420 K. For temperatures higher than 420 K ε′ decreases slowly indicating that a maximum is reached in the ε′ values. The 0.68PMN-0.32PT ceramics has a structural transition from cubic paraelectric to tetragonal ferroelectric symmetry at 420 K. Thus, it can be inferred that the maximum values observed in ε′ for all composites is related with the paraelectric–ferroelectric transition of the PMNPT phase in composites. The invariance of the ferroelectric phase transition temperature evidences the maintenance of PMNPT integrity in the composites form, independently of the sintering time (and average grain size). Additionally, the maximum values of dielectric permittivity, at 420 K, increases from values close to 12,500 to 25,000 and the phase transition diffuseness δ decreases with increasing average grain size, as seen in the Fig. 3b. Based on Eiras-Santos phenomenological model [22] the diffuseness parameter δ was obtained by the fit of the data with the Eq. (1). As observed in Fig. 3b, the diffuseness parameter δ decreases monotonically with the increment of the average grain size. This means that the phase transition is broader for composites with smaller ferroelectric grains than the coarser ones. According to the Mao et al. [23], a broader phase transition is generated when the phase transition is suppressed and, consequently, the maximum dielectric constant decreases. In ferroelectric ceramic systems, grain size changes affect the internal stress beside grains and the domains structures. When the grain size decreases, pinning points develop inside the grains and the domain wall motion is inhibited, reducing the tetragonal distortion and the dielectric permittivity of samples [18–20,23]. On the other hand, the internal stress, generated during the cubic-tetragonal phase transition, tends to suppress the spontaneous deformation, forcing the grains back to a cubic phase. In addition, *Jo* et al. [19] reported that changes in the average grain size could trigger the formation of the rhombohedral and

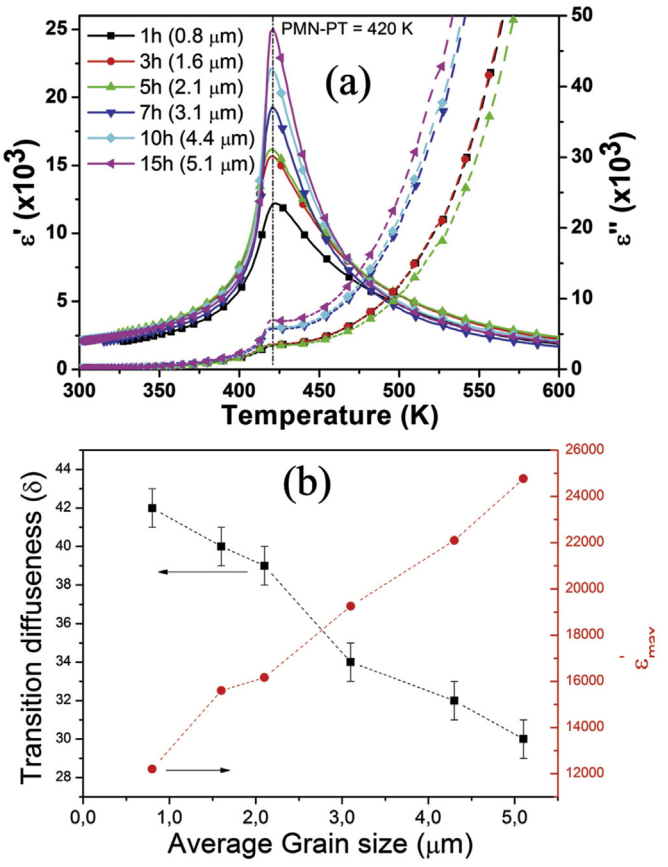

Figure 3. (a) Real (ε′) and imaginary (ε″) parts of electric permittivity, at 1 MHz, of PMNPT/CFO ME composite sintered at 1050 °C between 1 h and 15 h; and (b) transition diffuseness and maximum value of ε′ as a function of average grain size of PMNPT matrix.

tetragonal phases in case of the PMN-PT30 ferroelectric ceramics. This fact is generate by internal stress changes inside the grains. In this case, an increase of the dielectric permittivity values close to the phase transition was reported for samples with larger tetragonal concentration (average grain size larger than 1.4 μm), in comparison with samples with larger rhombohedral phase concentration (average grain size smaller than 1 μm). In front of discussed, it is possible to observe that our results indicate that the increase of grain size diminishes the internal stress enhancing the tetragonal distortion of PMNPT matrix and optimizing the dielectric properties of composites without change the phase transition temperature of composites.

Fig. 4 presents the magnetic hysteresis loops of the PMNPT/CFO magnetoelectric composites sintered at 1050 °C between 1 h and 15 h. As expected, it can be seen a ferromagnetic behavior, which the saturation magnetization reaches values close to 26 emu/g, independently of the sintering time. Moreover, the coercive field decreases 50% (from 160 Oe to 80 Oe) for samples sintered at long time (>5 h). Since the CFO molar content is the same for all samples, similar values for saturation magnetization independently of the sintering time is expected. In this case, the individual ferrite grains behave as centers of magnetization and the saturation magnetization of the composites is the sum vector of all of these individual contributions, where the ferroelectric phase does not change the nature of the magnetic interactions between the ferrite phase. On the other hand, a decrease in the coercive field with increasing the sintering time is related to the

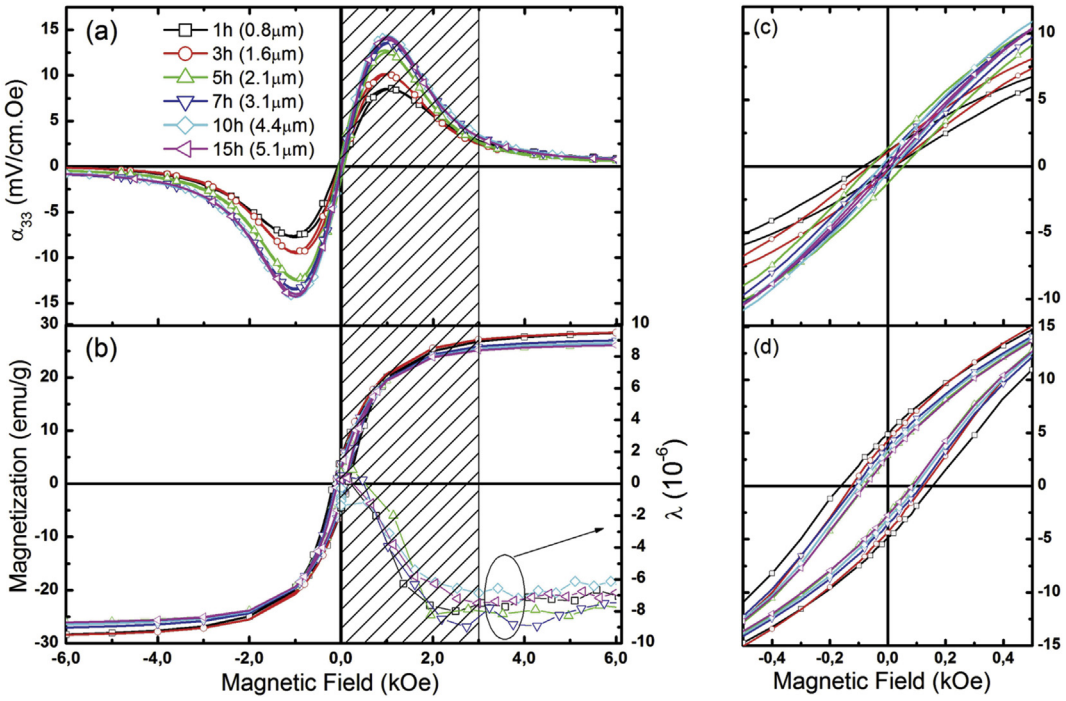

Fig. 4. (a) Magnetoelectric coefficient, α_{33} (and in the amplified scale (figure c)); and, (b) Magnetic hysteresis loop (and in the amplified scale (figure d)) and Magnetostriction measurements at room temperature as a function of magnetic applied field for PMN-PT/CFO sintered at 1050 °C, between 1 and 15 h.

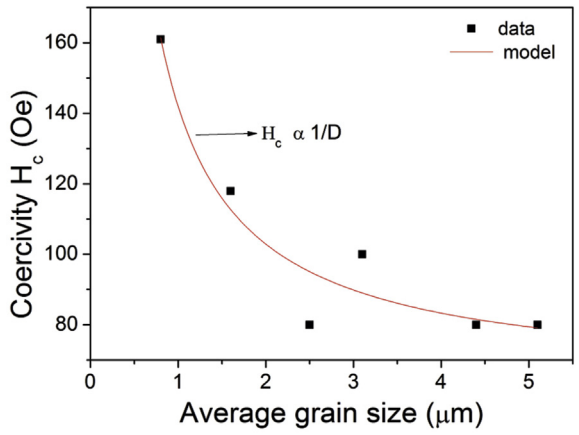

Fig. 5. Coercive field (Hc) as a function of average grain size of CFO phase in the composites sintered at different sintering time.

CFO grain size growth for long sintering time, as clearly seen in the Fig. 5. For large grains, the magnetization process can follow the easy magnetic directions in the single grains and domains can be formed within the grains in which the magnetization process is determined by magneto-crystalline anisotropy of the crystallites. In this case, the coercive field varies with 1/D law [24], where D is the average grain size of ferrite grains. As seen in the Fig. 5, our data of Hc indeed seem to match with expected 1/D law indicating an increase number of magnetic domain with increasing the grain size of CFO phase. This fact increases the number of domain walls decreasing the Hc since that the contribution of wall movement to magnetization is greater than that of domain rotation contribution.

The relative strain λ as a function of magnetic field for all composites is shown in the Fig. 4b. In agreement with magnetization, it is clear that strain λ reaches maximum values in the same magnetic field regions independently of grain size of composites in which is also associated to the domain reorientation as mainly contribution to the strain [25,26].

Fig. 4a shows the variation of the longitudinal ME voltage coefficient α_{33} as a function of the magnetic field for different PMNPT matrix grain size. The α_{33} coefficient shows maximum values for magnetic field around 1000 Oe and tend to zero for magnetic fields higher than 4 k Oe, in agreement to the maximum variation of magnetostrictive coefficient (indicated by gray region on the Fig. 4a and b).

In this case, the magnetostriction λ plays an important role in the shape of α_{33}, determining the magnetic field that the α_{ME} coefficient is maximum. Additionally, it is observed in the Fig. 4c a reduction of remnant α_{33} values (known as Self-biased ME values in composites) for samples with larger CFO grain size, in accordance to the remnant magnetization of the CFO phase in composites (observed in the Fig. 4d) and in agreement to the reported by Chen at al [27], which the zero bias magnetoelectric coefficient is achieved in magnetic phases that present non-zero piezomagnetic coefficient at $H_{dc} = 0$.

Considering the deformation occurring along the thickness direction and measuring the electric field along the same direction, the ME voltage coefficient can be expressed by Refs. [4,18]:

$$\alpha_E = m\left(\frac{dS}{dH}\right)_{ferrite} \times (1-m)(g_{33}C_{33})_{piezoelectric} \quad (2)$$

where m is the volume fraction of ferrite, dS/dH is the change in strain per unit magnetic field of ferrite in composite, g_{33} is piezoelectric voltage constant, and C_{33} is the stiffness of ferroelectric matrix into composite.

In our case, it is clear from the magnetic properties of

composites that the magnetostrictive term $\left(\frac{dS}{dH}\right)_{ferrite}$ and m are approximately constant, since it was held the integrity between phases during the sintering process. So, the changes in ME voltage coefficient with increment of PMNPT grain size could be related to the variation of the piezoelectric and mechanics coefficients of ferroelectric matrix. A comparison between the maximum value of the α_{ME} voltage coefficient and $g_{33}C_{33}$ product values as a function of the grain size is shown in the Fig. 6. The measured C_{33} value remains constant close to 16×10^{10} N/m^2, independently of average grain size, however, the g_{33} coefficient increases with grain size ones. The similar trend it is observed for α_{ME}. In our samples, the improvement of piezoelectric voltage coefficient g33 is attributed to the enhancement of tetragonal distortion in PMNPT phase due to control of the interfacial strain generated by refinement of grain size, in agreement to the structural and dielectrics results. From the Fig. 6 it is possible to observe an enhancing of the 65% in the ME coefficient (from 8.5 mV/cm Oe to 14.5 mV/cm Oe), controlling the dielectric and the piezoelectric properties of PMNPT phase in the composites through the improvement of tetragonal distortion of PMNPT. The maximum ME voltage coefficient of 7 mV/cm Oe has been reported [16] in PMNPT composite system, whereas the maximum ME coefficient values of 6 mV/cm Oe has been reported in CFO-PZT particulate composites system by Srinivasan et al. [28]. Recently, maximum ME voltage values between 0.2 and 10 mV/cm Oe has been reported in lead free particulate composites [29,30]. The maximum values observed for PMNPT/CFO in the present case are higher than that the previous reported values for similar magnetostrictive phases. In this sense, the control of internal stress of ferroelectric matrix by controlling the grain size during the sintering process is useful to obtain high-performance magnetoelectric composites in the particulate connectivity.

4. Conclusion

A serie of dense particulate composites constituted by (0.8)[0.675($Pb(Mg_{1/3}Nb_{2/3})O_3$)–0.325$PbTiO_2$] – (0.2)[$CoFe_2O_4$] were successfully prepared by solid-state sintering method, and the effects of grain size on structural, dielectric, magnetic, piezoelectric, magnetostrictive and magnetoeletric properties were systematically investigated. The values of ε', g_{33} and α_{ME} increased significantly with increasing grain size, reaching maximum values ($\varepsilon' = 25000$, $g_{33} = 53 \times 10^{-4}$ Vm/N and $\alpha_{ME} = 14.5$ mV/cm Oe) at approximately 4.5 μm. The coarsening of PMNPT matrix grain size diminishes the internal stress of grains increasing the tetragonal distortion of PMNPT phase that enhances the dielectric and piezoelectric properties of composites. As consequence, the changes of the piezoelectric properties induces an increase in the ME coupling values, which increases from 8 mV/cm Oe to ~14.5 mV/cm Oe for grain size between 0.8 μm and 5 μm. Additionally, the zero bias magnetoelectric field effect in the PMNPT/CFO composites related to the remnat magnetization was reported. The results revealed that high-performance magnetoelectric composite materials with particulate connectivity could be effectively prepared by controlling the structural properties through the grain size control during the sintering process.

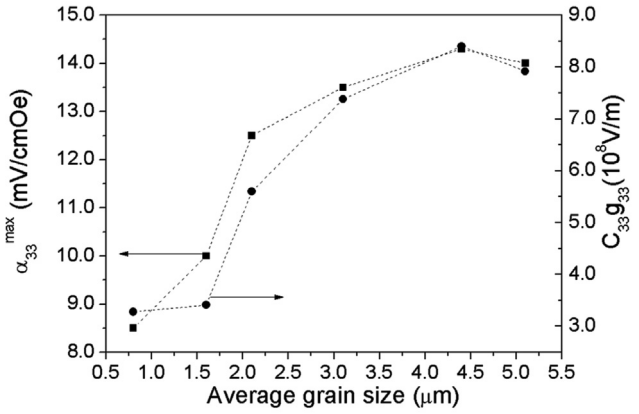

Fig. 6. Maximum value of α_{ME} coefficient; and, $c_{33}g_{33}$ product values of PMNPT/CFO particulate composites as a function of the PMNPT average grain size. Bias magnetic field up to 0.8T was applied overlapped by ac magnetic field of 2 Oe at 1 kHz.

Acknowledgments

The authors would like to thank Mr. Francisco José Picon and Mrs. Natália Aparecida Zanardi for the technical support, to Profa. Yvonne P. Mascarenhas (Crystallography Group of the Physics Institute of USP-São Carlos) for the use of the XRD Lab facilities, and FAPESP (Proc. 2008/04025-0, 2010/07518-7 and 2012/24025-0), Capes and CNPq (#477354/2013-0) for the financial support.

References

[1] W. Eerenstein, N.D. Mathur, J.F. Scott, Nature 442 (7104) (2006) 759.
[2] T. Lottermoser, T. Lonkai, U. Amann, D. Hohlwein, J. Ihringer, M. Fiebig, Nature 430 (6999) (2004) 541–544.
[3] J. Ryu, S. Priya, K. Uchino, H.E. Kim, J. Electroceram. 8 (2002) 107.
[4] C.W. Nan, M.I. Bichurin, S.X. Dong, D. Viehland, G. Srinivasan, J. Appl. Phys. 103 (2008), 10.1063.
[5] G.V. Duong, R. Groessinger, R.S. Turtelli, J. Magn. Magn. Mater. 310 (2007) 1157.
[6] K.K. Patankar, S.S. Joshi, B.K. Chougule, Phys. Lett. A 346 (2005) 337.
[7] R.S. Devan, B.K. Chougule, J. Appl. Phys. 101 (2007) 014109.
[8] R.A. Islam, S. Priya, Adv. Cond. Mat. Phys. (2012) 320612.
[9] R.C. Kambale, P.A. Shaikh, C.H. Bhosale, Y.D. Raipure, Y.D. Kolekar, J. Alloys Comp. 489 (2010) 310.
[10] A. Gupta, A. Huang, S. Shannigrahi, R. Chatterjee, Appl. Phys. Let. 98 (2011) 3562949.
[11] S. Priya, R. Islam, S.X. Dong, D. Viehland, J. Electroceram. 19 (2007) 147.
[12] Y. Zhou, F.G. Shin, J. Appl. Phys. 100 (2006) 043910.
[13] R.S. Devan, Y.D. Kolekar, B.K. Chougule, J. Alloy Comp. 461 (2008) 678.
[14] A.D. Sheikh, V.L. Mathe, Smart Mater. Struct. 18 (2009) 065014.
[15] A.D. Sheikh, V.L. Mathe, Mater. Chem. Phys. 119 (2010) 395.
[16] A.D. Sheikh, A. Fawzi, V.L. Mathe, J. Mag. Mag. Mater. 323 (2011) 740.
[17] F.L. Zabotto, A.J. Gualdi, A.J.A. Oliveira, J.A. Eiras, D. Garcia, Ferroelectrics 428 (2012) 122.
[18] R.A. Islam, S.J. Priya, Mat. Sci. 43 (2008) 3560.
[19] W. Jo, T.H. Kim, D. Kim, S.K. Pabi, J. Appl. Phys. 102 (2007) 2794377. Soc. 34(2014).
[20] W. Cai, C.L. Fu, J. Gou, H. Chen, J. Alloy Comp. 480 (2009) 870.
[21] Y.M. Yue, K.Y. Xu, T. Chen, Aifantis Phys. B Condens. Matter 478 (2015) 36–42.
[22] I.A. Santos, J.A. Eiras, J. Phys. Conden. Matter 13 (2001) 11733.
[23] C. Mao, S. Yan, S. Cao, C. Yao, F. Cao, G. Wang, X. Dong, X. Hu, C. Yang, J. Eur. Ceram. J. Eur. Soc. 34 (2014) 1529–1533.
[24] G. Herzer, IEEE Trans. Magn. 26 (5) (1990) 1397.
[25] N.N. Sarawate, M.J. Dapino, Smart Mater. Struct. 17 (2008) 065013.
[26] A.J. Moulson, J.M. Herbert, Electroceramics, 2nd. edn, John Wiley & Sons Ltd, Chichester, 2003.
[27] L. Chen, P. Li, Y. Wen, Y. Zhu, J. Alloy Comp. 606 (2014) 15.
[28] G. Srinivasan, R. Hayes, C.P. Devreugd, V.M. Laletsin, N. Paddubnaya, Appl. Phys. A 80 (2005) 891–897.
[29] H. Yang, G. Zhang, L. Ying, T. Ye, P. Kang, Ceram. Int. 41 (2015) 7227–7232.
[30] M.M. Sutar, S.R. Jigajemi, A.N. Tarale, S.B. Kulkarni, P.B. Joshi, J. Mater Sci. Electron. 25 (2014) 3771–3778.